

Direct preparation of macroporous mullite supports for membranes by in situ reaction sintering

Gangling Chen, Hong Qi, Weihong Xing*, Nanping Xu

State Key Laboratory of Materials-Oriented Chemical Engineering, Nanjing University of Technology, Nanjing 210009, PR China

Received 11 November 2007; received in revised form 10 January 2008; accepted 11 January 2008

Available online 31 January 2008

Abstract

The natural mineral kaolin combined with additive $\text{Al}(\text{OH})_3$ and AlF_3 as alumina sources was used to directly prepare macroporous mullite ceramic membrane supports through in situ reaction sintering. The effects of composition and the sintering temperature on the micro-morphology, phase development and pore structure of porous mullite support were investigated extensively. It was found that the excess SiO_2 in kaolin was consumed rapidly by adding the alumina precursors with the formation of secondary mullite in the temperature range of 1300–1500 °C. During the sintering process, pore structure and stiff skeleton needle-like structure mullite formed in the support, which resulted in good pore structure and high mechanical strength. Thus, the support is suitable for the preparation of asymmetric ceramic membranes. The pore structure and the micro-morphology of the support could be controlled by adjusting raw material Al_2O_3 composition from 50 to 72 wt.% of Al_2O_3 and the sintering temperature from 1300 to 1550 °C. The porous mullite supports with the porosity of 27–55.6%, average pore size of 0.73–1.50 μm and mechanical strength of 15.5–66.7 MPa were prepared after optimization.

© 2008 Published by Elsevier B.V.

Keywords: Support; Needle-like mullite; Reaction sintering; Ceramic membrane

1. Introduction

Ceramic membranes have been known for years and applied in many industrial processes due to their advantages, such as high separation efficiency, excellent thermal stability, high-pressure resistance, chemical stability, and long life [1–3]. The support is known as a key part of asymmetric ceramic membrane, which provides mechanical strength and flow transport for the top-layer membrane [4]. Hereinto, alumina is considered as the main support material of commercialized ceramic separation membranes. However, due to the expensive raw material and high cost of sintering in the production of Al_2O_3 support, Al_2O_3 support-based membranes are too expensive when used in some economical separation processes [5,6]. As a result, in recent years, the preparation and potential applications of porous mineral-based ceramic membrane have increasingly attracted attention due to the low cost in the raw material available from natural mineral [5–12].

Kaolin was well studied in the past decades for serving the conventional ceramics. However, there have been renewed interests in the conversion of kaolin to mullite ($3\text{Al}_2\text{O}_3 \cdot 2\text{SiO}_2$) for preparing the membrane material in filtration [9–16] owing to its low cost and relatively low sintering temperature. A grave problem, however, is that the mullite support made by the conventional method is generally dense due to the excess SiO_2 existing in kaolin. In general, the pores were produced by leaching out the excess silica from fired clays or the resulted product with the solutions, such as NaOH [13,14], acid [15] and caustic potash [17]. In order to achieve rapid and complete leaching, some processes were completed even under the hydrothermal and microwave conditions [16]. The added complexity of leaching in the processing is undesirable. Furthermore, the reported average pore size and the open porosity obtained by these methods are 0.17–0.61 μm and 40–57%, respectively [12]. The pore sizes are smaller than those desirable for the filtration applications. In order to provide a solution to this problem, Al_2O_3 powders have been proposed to be added. The addition of Al_2O_3 powders can reduce the amount of glass phase (SiO_2) and increase the amount of mullite. In the present investigation, a new processing route was applied to directly make porous

* Corresponding author. Tel.: +86 25 8358 7718; fax: +86 25 8330 0345.
E-mail address: xingwh@njut.edu.cn (W. Xing).

mullite supports using the additive of suitable alumina precursors. It is expected that while the excess SiO_2 in kaolin is consumed by the additive alumina precursors, the pore structure and stiff skeleton needle-like structure mullite [18] forms in situ, which would make support have a good pore structure and high strength [18–20].

This work aims to examine the effects of the composition and the sintering temperature on the microstructure, phase development and pore structure of porous support made by the proposed processing route.

2. Experimental

2.1. Sample preparation

Kaolin (China Kaolin Company) and industrial $\text{Al}(\text{OH})_3$ powder were used as the starting materials and AlF_3 was used as an additive. The composition of the starting materials was determined by the Switzerland ARL9800XP X-ray fluorescence spectrometer. The mixtures of the starting powders with different content of alumina precursor were ball-milled together. The grinding media was corundum balls and milling time was 12 h. Some binders and lubricant were added to the mixed powder. The powder compacts were prepared by press molding technique. The pressure applied was 8 MPa. The firing was carried out under different temperature from 1300 to 1550 °C for 2 h with the heating rate of 3 °C min^{-1} in a programmable electric furnace.

2.2. Characterizations

The microstructure of sintered samples were analyzed by scanning electron microscopy (SEM, Quanta 200, FEI, Netherlands) with an energy dispersive X-ray spectrometer (EDX). Phase analysis of the sintered samples was identified by X-ray diffraction (XRD, D8 advance, Bruker Instrument Co., Ltd. Germany). In order to determine the amount of mullite content in the sintered samples, a high-purity mullite was used to mix the alumina powder. The integrated intensity of the (1 2 1) reflection (2θ from 40.5° to 41.5°) of the high-purity mullite powder was used as the standard for determining the mullite content. Open porosity was determined by the Archimedes method (GB1996-80) with water as the liquid medium. Average pore size and pore size distribution (PSD) of the sintered porous specimen were measured using the gas bubble pressure method (GBP), which was performed following the American Society for Testing and Materials (ASTM) Publication (F316-80). The flexural strengths were measured by a three-point bending test with a support distance of 40 mm and a cross-head speed of 0.5 mm min^{-1} .

3. Results and discussion

3.1. X-ray diffraction investigations

The samples with different Al_2O_3 contents were sintered at 1500 °C for 2 h, and the XRD patterns of samples are shown in Fig. 1. The samples containing 50 wt.% Al_2O_3 and contain-

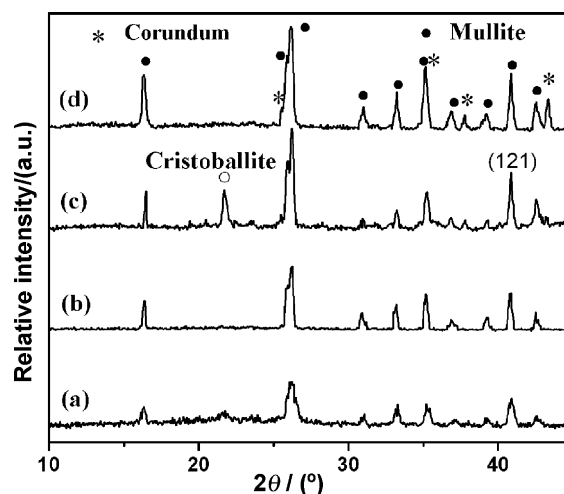


Fig. 1. XRD patterns of the samples sintered at 1500 °C for 2 h with various Al_2O_3 content of (a) kaolin, (b) 50, (c) 60 and (d) 72 wt.%.

ing mere kaolin show complete orthorhombic mullite diffraction peaks, the later is accompanied with the heavy background due to the existence of silica glassy phases which formed from the decomposition of kaolin. For the samples with 60 wt.% Al_2O_3 , however, not only mullite but also a little cristobalite and corundum co-existed in sample. The samples consisting of 72 wt.% Al_2O_3 mixtures, however, not only mullite but also corundum formed in the fired samples. The results indicated that phase compositions of the sintered supports could be tuned by alumina precursor content.

In order to understand the reaction mechanism, the green samples with 60 wt.% Al_2O_3 and the pure kaolin samples were sintered at 1300, 1400, 1500 and 1550 °C for 2 h separately for comparison. The XRD patterns and mullite contents are shown in Figs. 2 and 3, respectively. Fig. 2 shows the XRD patterns of the samples with 60 wt.% Al_2O_3 as sintered at 1300–1550 °C for 2 h. It can be seen that the final phase compositions depended greatly on the sintering temperature. The intensity of mullite phase increased because of the formation of mullite when the

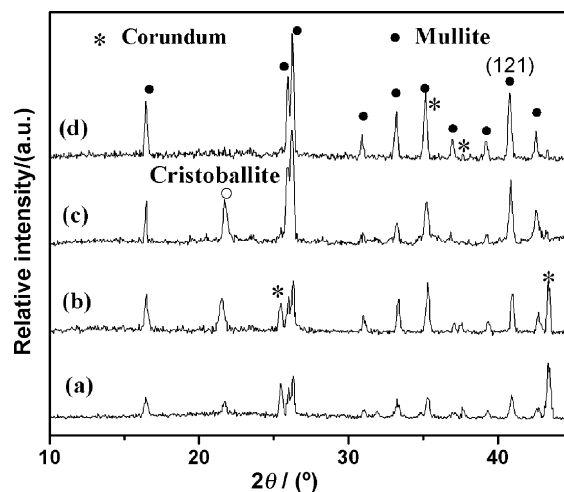


Fig. 2. XRD patterns of the samples (60 wt.% Al_2O_3) as sintered at (a) 1300, (b) 1400, (c) 1500 and (d) 1550 °C for 2 h.

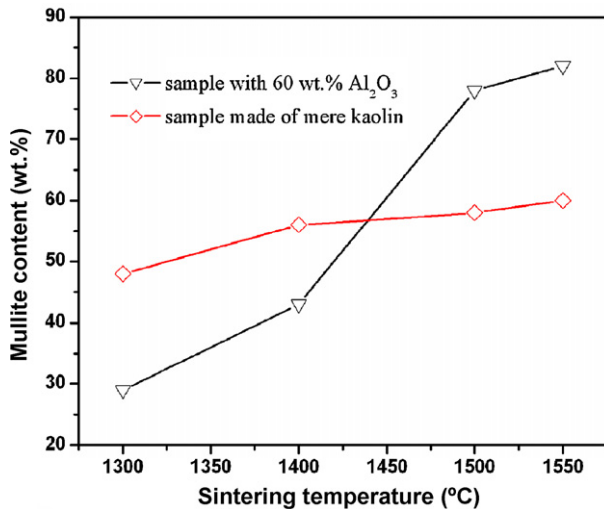
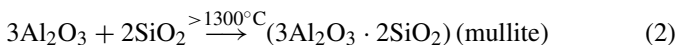
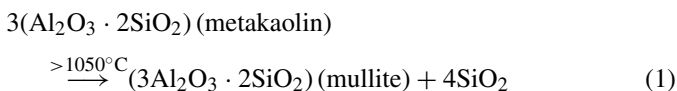


Fig. 3. Effect of sintering temperature on content of mullite in samples.

sintering temperature increased by examining the target reflection (1 2 1). Al₂O₃ peaks almost disappeared at the 1550 °C. The cristobalite phase was also undetectable at the temperature above 1500 °C, which might dissolve into glassy phase and contribute to the formation of mullite phase.

Fig. 3 shows the dependence of mullite phase content of the sintered samples on the sintering temperature. The mullite content in the sintered sample made of mere kaolin increased slowly from 48.2 to 60.3 wt.% when the sintering temperature increased from 1300 to 1550 °C due to the gradual transformation of kaolin. On the other hand, in the sintering temperature range from 1300 to 1500 °C, the mullite content in sample with additive Al₂O₃ increased rapidly from 29.1% to 82.3%, especially, at temperatures between 1400 and 1500 °C. The increase in mullite content in this temperature range is due to the formation of secondary mullite [21]. The content of mullite did not show significantly increase at the temperature above 1500 °C. It can be also learned from Fig. 3 that the glass phase was consumed rapidly with the formation of secondary mullite in the temperature region from 1300 and 1500 °C. In summing up, the excess SiO₂ in kaolin can be consumed by adding alumina precursors and increase the amount of mullite, which is beneficial to obtain porous mullite support. This can be explained by the following reactions [22]:



3.2. The microstructure of sintered samples

The microstructure of samples sintered at 1500 °C for 2 h with different Al₂O₃ contents are shown in Fig. 4. Fig. 4a displays the microstructure of the sample with 50 wt.% Al₂O₃, a large quantity of continuous glassy phases remained in the sample, in which small pores and needle-like mullite are embedded. According to

the XRD patterns shown in Fig. 1, the main phase in Fig. 4a was mullite phase. For the sample with 60 wt.% Al₂O₃ (Fig. 4b), large pores with mullite whisker clumps were clearly observed. The whiskers could form a short network, which acted as a skeleton of pore structure. Similar morphology had been observed by Mohamed et al. [23]. Comparing with the sample with 60 wt.% Al₂O₃, the samples with 65–72 wt.% Al₂O₃ content, as shown in Fig. 4c–d, respectively, there were fewer needle-like structure mullite grains present in the sintered support. However, the porosity increased gradually with the increase of alumina content, as will be further discussed in the following sections. The results reveal that for silica-rich mullite, the grains tend to be needle-like, and aluminum-rich samples, round particles appear, being similar to that of the previous studies [24,25]. For the low-alumina sample, the excess liquid glassy phase of low viscosity promoted the formation of needle-like mullite crystals. Additionally, during the formation of mullite the alumina grains act as the nuclei for the formation of mullite [26,27]. The increase of Al₂O₃ content in sample not only increases the amount of nuclei centers but also decreases the amount of liquid glassy phase due to mullitization. As a result, for the high alumina sample, granulated crystals were produced.

In order to investigate the microstructure evolution of samples during the sintering process, the samples with 60 wt.% Al₂O₃ content sintered at various temperatures for 2 h were examined by SEM. The results are shown in Fig. 5. From Fig. 5(a), it is found that the Al₂O₃ particles dispersed in the glassy phase with the primary mullite [28] formed from the kaolin phase transformation at the temperature of above 1000 °C. The Al₂O₃ particles, SiO₂ and mullite further mixed up in submicrometer and micrometer size scale as the sintering temperature increased, as can be seen from Fig. 4(b). The Al₂O₃ dissolved into the glassy phase for second formation of mullite [21]. Based on the results of Figs. 2 and 3, we therefore speculate that the Al₂O₃ and SiO₂ first formed an amorphous aluminosilicate phase that simply surrounded the primary mullite particles. While the reaction between Al₂O₃ and SiO₂ went on, the mullite crystals grown up. The excess SiO₂ in kaolin was thus consumed rapidly with the rapid formation and growth of mullite in the temperature range of 1400–1500 °C. When the free glassy phase are consumed, stiff skeleton needle-like structure mullite formed in situ, which provided a good pore structure, as can be seen from Figs. 3b and 4d.

3.3. Pore parameters of sintered samples

3.3.1. Porosity

The effect of the Al₂O₃ content and the sintering temperature on the porosity of the samples is illustrated in Fig. 6. It can be found from Fig. 6 that in all cases, porosity increases as the Al₂O₃ content in specimens increases from 50 to 72 wt.%. The more the Al₂O₃ content presented in samples, the higher is the porosity at the same sintering temperature (1300–1550 °C). The result could be due to the fact that the content of Al₂O₃ from kaolin is less than 46 wt.%, and the rest in samples mainly comes from the decomposition of additive Al(OH)₃. The in situ decomposition of Al(OH)₃ produced 60% volume contraction

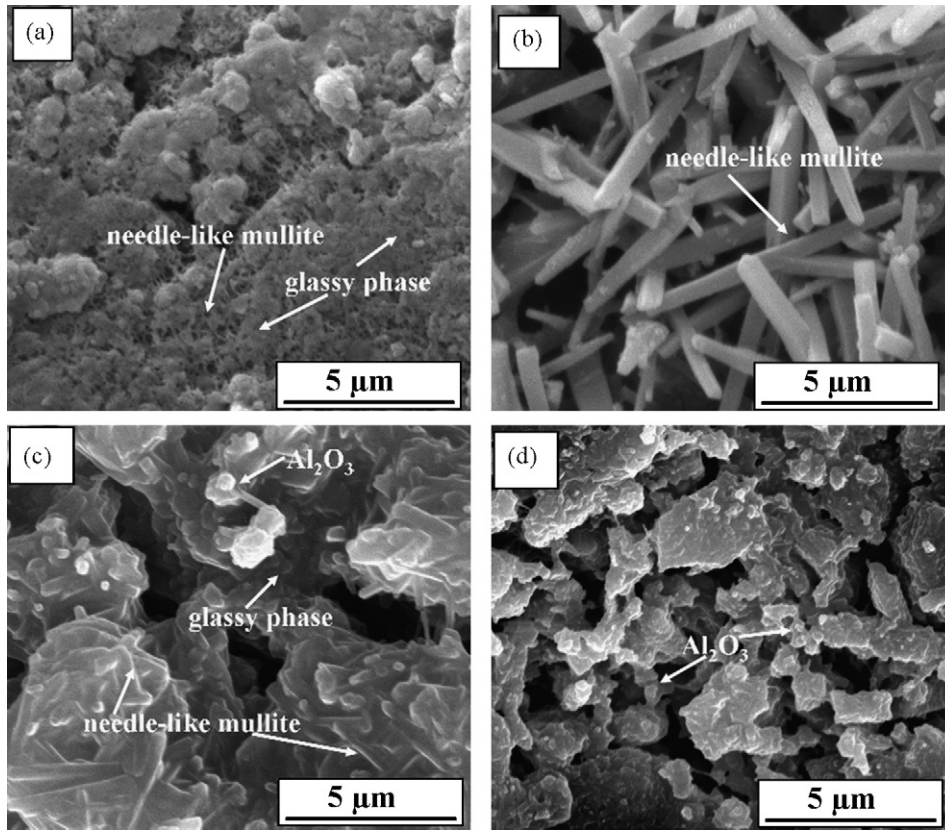


Fig. 4. SEM photos of samples sintered at 1500 °C for 2 h with various Al₂O₃ content (a) 50, (b) 60, (c) 65 and (d) 72 wt.%.

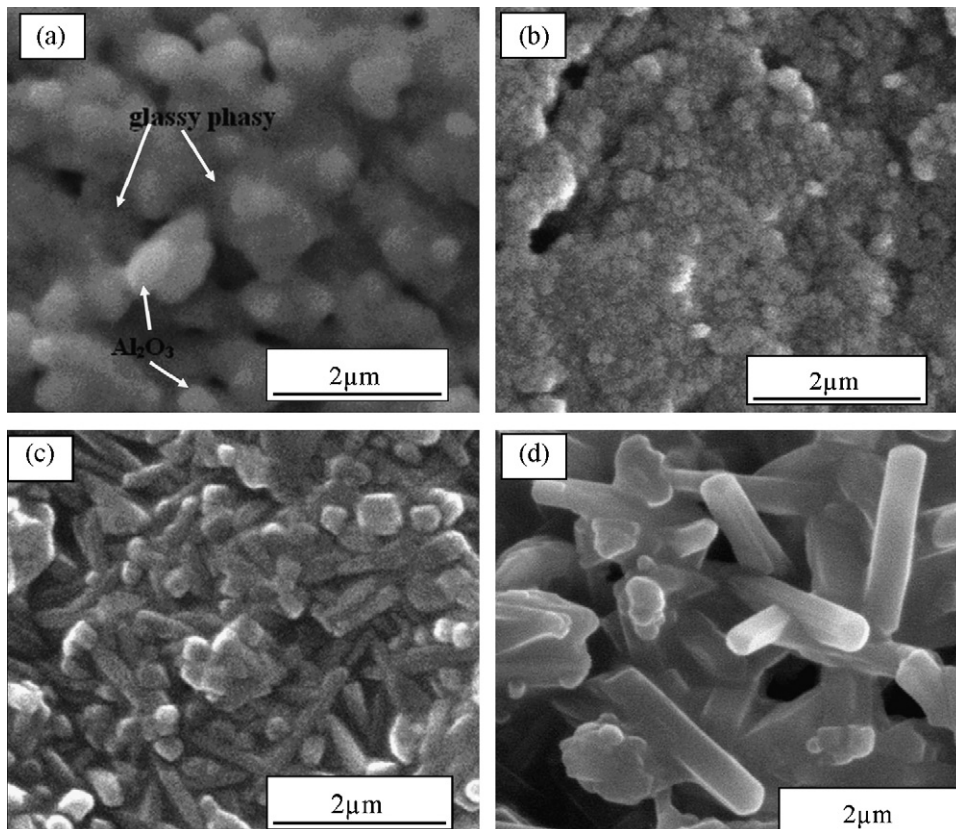


Fig. 5. SEM photos of the samples with 60 wt.% Al₂O₃ sintered at (a) 1300, (b) 1400, (c) 1450 and (d) 1550 °C for 2 h.

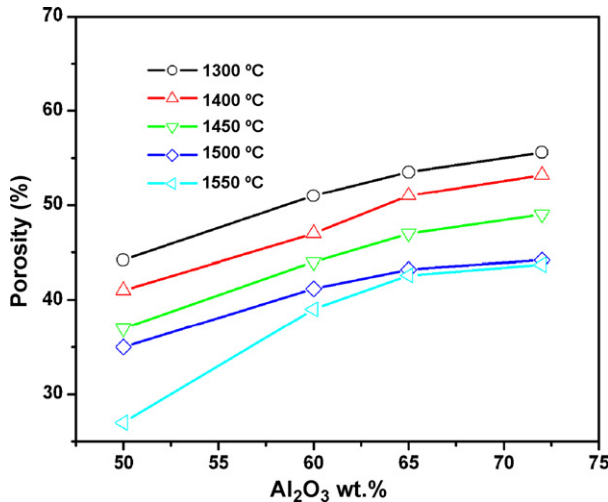


Fig. 6. Porosity of the samples with different Al_2O_3 wt.% sintered at different temperatures.

[29] and left some space around the Al_2O_3 particles. Thus, an increase of apparent porosity was observed when increasing the Al_2O_3 content (Fig. 6). It is also found from Fig. 6 that all the porosity decreased as the sintering temperature increased. When Al_2O_3 content was above 60 wt.%, the porosity achieved at 1500–1550 °C was less dependent on the sintering temperatures.

3.3.2. Average pore sizes and pore size distribution

The pore size distributions of the samples sintered at 1500 °C for 2 h are shown in Fig. 7. As shown, in the samples with Al_2O_3 content of 50–65 wt.%, as Al_2O_3 wt.% rose, the average pore size increased gradually, and the average pore sizes of the samples with 50, 60 and 65 wt.% Al_2O_3 were 0.73, 1.16 and 1.50 μm , respectively. However, as the Al_2O_3 content reached 72 wt.%, the average pore size of the sample decreased and it became 1.02 μm . Comparing to the analysis of the SEM photos of sample shown in Fig. 4, the pores with various sizes might be influenced by three possible factors: (a) the silica glassy phase formed from the decomposition of metakaolin, (b) stiff skeleton needle-like structure mullite formed in the secondary mullitization and (c) residual Al_2O_3 from the decomposition of $\text{Al}(\text{OH})_3$. During the sample calcination, the formation of stiff skeleton needle-like structure mullite was very favorable to enlarge the

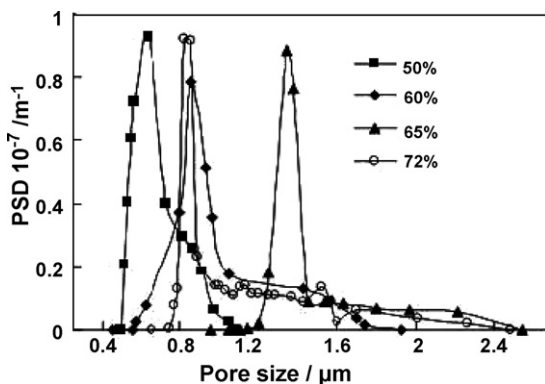


Fig. 7. Pore size distributions of the samples sintered at 1500 °C for 2 h.

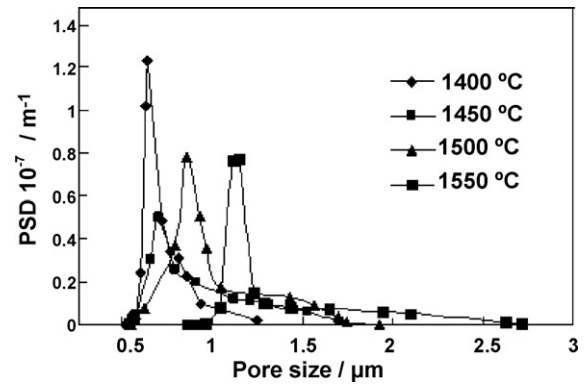


Fig. 8. Pore size distributions of the samples with 60 wt.% Al_2O_3 sintered at different temperatures.

pore size and inhibit the shrinkage of sample. For the samples with low Al_2O_3 content, there were large free glassy phase, which caused a large sintering shrinkage with the result of small pore size. This can be confirmed by the sample with 50 wt.% Al_2O_3 . For the samples with higher Al_2O_3 content, however, the amount of Al_2O_3 was more than the need to react with free glassy phase. The residual fine Al_2O_3 particles came from the in situ decomposition of $\text{Al}(\text{OH})_3$ [29]. During the sintering, the residual part fine Al_2O_3 grains diffused into the large pore of support, as can be observed from the SEM photo (Fig. 4d) of sample with 72 wt.% Al_2O_3 and lead to a reduced pore size, as can be confirmed from the sample with 72 wt.% Al_2O_3 .

Fig. 8 illustrates the dependence of pore size distribution on sintering temperature of the sintered sample with 60 wt.% Al_2O_3 . It is found that the pore size distributions of the sample are closed related to the sintering temperature. The average pore size increases as the sintering temperature increases, and the values were 0.74, 0.96, 1.16 and 1.52 μm for 1400, 1450, 1500, and 1550 °C, respectively. When the samples were sintered at higher temperature, more big pores larger than 1.5 μm appeared in the sample, as can be seen from Fig. 8. This attributed to the formation and growth of stiff skeleton needle-like structure mullite. Meantime, as the sintering temperature increased the excess glassy silica in the samples was consumed by mullitization reaction, which was beneficial to enlarge the pore size. This can be confirmed by the pore size distribution of the specimen sintered at 1550 °C, as shown in Fig. 8. The pore size evolution was consistent with the results of XRD analysis (Fig. 2) and the microstructure evolution (Fig. 5).

According to the results in Figs. 7 and 8, it was suggested that the mean pore size and pore size distribution should be able to be controlled by adjusting the composition and the sintering temperature of sample.

3.4. Three-point bending strength of samples

Fig. 9 shows the three-point bending strength of supports sintered at different temperatures (1300–1550 °C). The strength was enhanced with the increase of sintering temperature in the range of 1300–1550 °C. When the sintering temperature was above 1450 °C, the strength of samples increased abruptly from

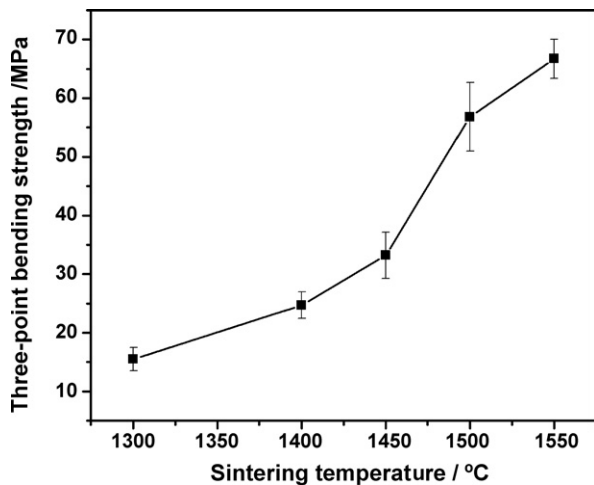


Fig. 9. Strength of samples with 60 wt.% Al_2O_3 sintered at different temperatures.

33.2 to 66.7 MPa. This could be attributed to the formation and growth of needle-like structure mullite and the reduction of glassy phase [27], as can be also deduced from Figs. 3 and 4. In this work, AlF_3 was used as the additive precursor. During the formation of mullite, AlF_3 acted as a kind of catalyst, which promoted the formation of needle-like mullite [30,31]. The intergrown needle-like mullite crystals could impart mechanical strength and structure rigidity to the porous mullite support.

4. Conclusions

The natural mineral kaolin with additive $\text{Al}(\text{OH})_3$ and AlF_3 as alumina source was used to directly prepare porous mullite supports through in situ reaction sintering. During the sintering, pore structure and stiff skeleton needle-like structure mullite formed in situ, which produced a good pore structure and high mechanical strength in the support. The excess SiO_2 in kaolin was consumed rapidly with additive alumina precursors accompanying with the formation of secondary mullite in the temperature range of 1300–1500 °C. The microstructure of support was strongly related to both Al_2O_3 content and sintering temperature. The properties of porous mullite support (porosity, average pore size, phase composition, the micro-morphology and mechanical strength) can be controlled by adjusting the preparation conditions (e.g. raw material composition and the sintering temperature). The porous mullite supports with the porosity (27–55.6%), average pore size (0.73–1.50 μm) and mechanical strength (15.5–66.7 MPa) were prepared after optimization.

Acknowledgements

This work was supported by the National Basic Research Program of China (No. 2003CB615707), the National Natural Science Foundation of China (No. 20436030), the National High Technology Research and Development Program of China (No. 2006AA03Z534), and the NCET.

References

- [1] N.P. Xu, Process-Oriented Design, Preparation and Application of Ceramic Membrane, Science Press, Beijing, 2005.
- [2] K.A. DeFriend, A.R. Barron, A simple approach to hierarchical ceramic ultrafiltration membranes, *J. Membr. Sci.* 212 (2003) 29–38.
- [3] B. Elyassi, M. Sahimi, T.T. Tsotsis, A novel sacrificial interlayer-based method for the preparation of silicon carbide membranes, *J. Membr. Sci.* 316 (2008) 73–79.
- [4] P.M. Biesheuvel, H. Verweij, Design of ceramic membrane supports: permeability, tensile strength and stress, *J. Membr. Sci.* 156 (1999) 141–152.
- [5] Y.C. Dong, X.Q. Liu, Q.L. Ma, G.Y. Meng, Preparation of cordierite-based porous ceramic micro-filtration membranes using waste fly ash as the main raw materials, *J. Membr. Sci.* 285 (2006) 173–181.
- [6] S. Masmoudi, A. Larbot, H. El Feki, R. Ben Amar, Elaboration and characterisation of apatite based mineral supports for microfiltration and ultrafiltration membranes, *Ceram. Int.* 33 (2007) 337–344.
- [7] M.C. Almandoz, J. Marchese, P. Prádanos, L. Palacio, A. Hernández, Preparation and characterization of non-supported microfiltration membranes from aluminosilicates, *J. Membr. Sci.* 241 (2004) 95–103.
- [8] Y.C. Dong, X.Y. Feng, D.H. Dong, Elaboration and chemical corrosion resistance of tubular macro-porous cordierite ceramic membrane supports, *J. Membr. Sci.* 304 (2007) 65–75.
- [9] A. Belouatek, N. Benderdouche, A. Addou, A. Ouagued, N. Bettahar, Preparation of inorganic supports for liquid waste treatment, *Microporous Mesoporous Mater.* 85 (2005) 163–168.
- [10] Y.F. Liu, X.Q. Liu, G. Li, G.Y. Meng, Low cost porous mullite-corundum ceramics by gelcasting, *J. Mater. Sci.* 36 (2001) 3687–3692.
- [11] F. Bouzerara, A. Harabi, S. Achour, A. Larbot, Porous ceramic supports for membranes prepared from kaolin and dolomite mixtures, *J. Eur. Ceram. Soc.* 26 (2006) 1663–1671.
- [12] Y.F. Liu, X.Q. Liu, H. Wei, G.Y. Meng, Porous mullite ceramics from national clay produced by gelcasting, *Ceram. Int.* 27 (2001) 1–7.
- [13] A. Pak, T. Mohammadi, Dehydration of water/1-1-dimethylhydrazine mixtures by zeolite membranes, *Microporous Mesoporous Mater.* 70 (2004) 127–134.
- [14] H. Katsuki, S. Furuta, A. Shiraishi, S. Komameni, Porous mullite honeycomb by hydrothermal treatment of fired kaolin bodies in NaOH, *J. Porous Mater.* 2 (1996) 299–305.
- [15] H. Katsuki, H. Takagi, O. Matsuda, Fabrication and properties of mullite ceramics with needle-like crystals, *Ceram. Trans.* 31 (1992) 137–146.
- [16] H. Katsuki, S. Furuta, S. Komameni, Conventional versus microwave-hydrothermal leaching of glass from sintered kaolinite to make porous mullite, *J. Porous Mater.* 3 (1996) 127–131.
- [17] Y. Saito, S. Hayashi, A. Yasumori, K. Okada, Effect of calcining conditions of kaolinite on pore structures of mesoporous materials prepared by selective leaching of calcined kaolinite, *J. Porous Mater.* 3 (1996) 233–239.
- [18] K. Okada, N. Otsuka, Synthesis of mullite whiskers and their application in composites, *J. Am. Ceram. Soc.* 74 (1991) 2414–2418.
- [19] H. Shin, C.S. Kim, S.N. Chang, Mullitization from a multicomponent oxide system in the temperature range 1200–1500 °C, *J. Am. Ceram. Soc.* 83 (2000) 1237–1240.
- [20] Y.F. Chen, M.C. Wang, M.H. Hon, Pore structure and permeation properties of kaolin–silica–alumina ceramics, *J. Ceram. Soc. Jpn.* 111 (2003) 537–543.
- [21] Y.F. Chen, M.C. Wang, M.H. Hon, Kinetics of secondary mullite formation in kaolin– Al_2O_3 ceramics, *Scripta Mater.* 51 (2004) 231–235.
- [22] Y.F. Chen, M.C. Wang, M.H. Hon, Phase transformation and growth of mullite in kaolin ceramics, *J. Eur. Ceram. Soc.* 24 (2004) 2389–2397.
- [23] G. Mohamed, M.U. Ismail, A. Hiroshi, N. Zenzira, A. Tokuji, Mullite whiskers from precursor gel powders, *J. Am. Ceram. Soc.* 73 (1990) 2736–2739.
- [24] T. Kumazama, Influence of Chemical composition on the mechanical properties of SiO_2 – Al_2O_3 ceramic, *J. Ceram. Soc. Jpn. (Int. Ed.)* 96 (1988) 85–91.
- [25] Y.F. Chen, M.C. Wang, M.H. Hon, Transformation kinetics for mullite in kaolin– Al_2O_3 ceramics, *J. Mater. Res.* 18 (2003) 1355–1362.

- [26] D. Papargyris, R.D. Cooke, Structure and mechanical properties of kaolin based ceramics, *Br. Ceram. Trans.* 95 (1996) 107–120.
- [27] C.Y. Chen, G.S. Lan, W.H. Tuan, Preparation of mullite by the reaction sintering of kaolinite and alumina, *Eur. Ceram. Soc.* 20 (2000) 2519–2525.
- [28] M. Panneerselvam, K.J. Rao, Novel microwave for the synthesis and sintering of mullite from kaolinite, *Chem. Mater.* 15 (2003) 2247–2252.
- [29] Z.Y. Deng, T. Fukasawa, M. Ando, Microstructure and mechanical properties of porous alumina ceramics fabricated by the decomposition of aluminum hydroxide, *J. Am. Ceram. Soc.* 84 (2001) 2638–2644.
- [30] H.J. Choi, J.G. Lee, Synthesis of mullite whiskers, *J. Am. Ceram. Soc.* 85 (2002) 481–483.
- [31] Y.J. Chen, B. Chi, Q.X. Liu, D.C. Mahon, Fluoride-assisted synthesis of mullite($\text{Al}_{5.65}\text{Si}_{0.35}\text{O}_{9.175}$) nanowires, *Chem. Commun.* 26 (2006) 2780–2782.